THE JOURNAL OF PHYSICAL CHEMISTRY C

Article

pubs.acs.org/JPCC

Large Piezoelectric Response Induced by the Coexistence of Low-Symmetry and Self-Polarization in Li^+-Nb^{5+}-Doped $BiFeO_3$ Polycrystalline Films

Yafei Hou,[†] Weili Li,[†,‡] Tiandong Zhang,[†] WenPing Cao,[†] Yang Yu,[†] Tergul Bai,[†] and Weidong Fei*[,†]

[†]National Key LAB for Advanced Welding and Joining, Harbin Institute of Technology, Harbin 150001, P.R. China

[‡]National Key Laboratory of Science and Technology on Precision Heat Processing of Metals, Harbin Institute of Technology, Harbin 150001, People's Republic of China

ABSTRACT: Pure $BiFeO_3$ (S1) and Li^+-Nb^{5+}-pair-doped $BiFeO_3$ (S2, S3, and S4) films were prepared by the radio-frequency magnetron sputtering onto the $LaNiO_3$-buffered Pt/Ti/SiO_2/Si substrate. The phase structure of the doped $BiFeO_3$ films is low-symmetry T-like phase owing to the chemical pressure induced by the substitution of larger Li^+ and Nb^{5+} for smaller Fe^{3+}, which is different from the pure $BiFeO_3$ film (high-symmetry R phase). Compared with the pure $BiFeO_3$ film, the dielectric, ferroelectric, and piezoelectric performances are greatly enhanced, especially for the piezoelectric response of 9 wt % Li^+-Nb^{5+}-doped $BiFeO_3$ (S3) film. The converse piezoelectric coefficient d_{33} of S3 film is 114.1 pm/V, which is comparable to that of lead-based piezoelectric films. The excellent piezoelectricity of S3 film is considered as the coupling results of low-symmetry T-like phase $BiFeO_3$ and upward self-polarization because the polarization vectors of the T-like phase and nanodomains rotate easily under small external stimuli. In addition, the reduced leakage currents in the doped $BiFeO_3$ films also contribute to the enhanced dielectric, ferroelectric, and piezoelectric performances.

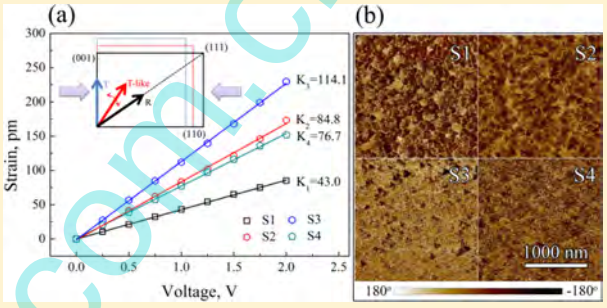

1. INTRODUCTION

With the development of microelectromechanical and transducer applications, ferroelectric materials with superior piezoelectric responses have been of great interest among researchers.[1−5] Large piezoelectric responses are usually relevant to the morphotropic phase boundaries (MPBs), as is observed in lead-based ferroelectrics.[6−8] Among the lead-free candidates, the epitaxial $BiFeO_3$ thin films with strain-driven MPB and low-symmetry tetragonal- and rhombohedral-like (T- and R-like) phases have spurred great interest recently.[9−13] Around the MPB, the relatively small-energy barriers between the low-symmetry phases, whose spontaneous polarization vector can rotate freely within a monoclinic plane, make them very susceptible to external electric field or stress, leading to a large piezoelectric response.[14−16] Thus, $BiFeO_3$ provides an alternate choice for the future applications as a "green" piezoelectric material.

Apart from the mismatch stress in the epitaxial $BeFeO_3$ thin films, the phase transition of pure $BiFeO_3$ from R phase to another low-symmetry phase can also be triggered by ion substitutions, displaying an MPB characteristic with enhanced ferroelectric and piezoelectric response.[17−20] Furthermore, it has been reported that the high leakage current density can be greatly reduced by the introduction of Mn, Ti, and Nb ions into Fe site to eliminate oxygen vacancies[21−23] or the insertion of a buffer layer to prevent the interfacial reaction between platinum and bismuth.[24−26] The reduced leakage current is of benefit in applying higher electric fields and switching domains so that an enhanced ferro/piezoelectric response can be expected;[27−29] however, the ion substitution in the past has been confined to single ion doping, while ion-pair doping at the same site has rarely been reported in the $BiFeO_3$ polycrystalline film.

Furthermore, the self-polarization phenomenon (macroscopic polarization without external electric field), where the high orientation is generally needed,[30,31] is also considered to be responsible for large piezoelectric response because the rotation of polarization vector is easy to be realized under an external stimuli.[32,33] On the basis of our previous reports, the optimized distribution of doped ion-pairs parallel to the (001) direction can also lead to a large piezoelectric response.[34,35] Besides, the electric field induced by directional arrangement of ion pairs could be helpful to realize the self-polarization. In the present study, Li^+-Nb^{5+}-doped $BiFeO_3$ polycrystalline films with large piezoelectric response and upward self-polarization were prepared by the radio-frequency magnetron sputtering, and $LaNiO_3$ was used as the buffer layer to induce the high (001) orientation and prevent the direct contact of $BiFeO_3$ and Pt. For comparison, four films with different Li^+-Nb^{5+} pair contents have been prepared via the same method. In addition, the effect of Li^+-Nb^{5+} pair, $LaNiO_3$ buffer layer, and the mechanism of large piezoelectric response in Li^+-Nb^{5+}-pair-doped $BiFeO_3$ polycrystalline films are discussed.

Received: December 15, 2015
Revised: March 7, 2016
Published: March 9, 2016

ACS Publications © 2016 American Chemical Society

DOI: 10.1021/acs.jpcc.5b12291
J. Phys. Chem. C 2016, 120, 6246−6251

www.spm.com.cn

2. EXPERIMENTAL SECTION

The polycrystalline films of pure $BiFeO_3$ and doped $BiFeO_3$ with different Li^+-Nb^{5+} pair contents were prepared by the radio frequency magnetron sputtering using the $BiFeO_3$ target with different $LiNbO_3$ pellets. The $LiNbO_3$ pellets were pasted on the $BiFeO_3$ target with silver pastes. The $LaNiO_3$ buffer layer was introduced on the $Pt/Ti/SiO_2/Si$ substrate using a sol−gel technique before the growth of $BiFeO_3$ film, as previously reported.[36] A base pressure of 5.0×10^{-4} was achieved in the deposition chamber and the $BiFeO_3$ target with $LiNbO_3$ pellets was presputtered for 15 min to eliminate the surface heterogeneity. The depositions of pure $BiFeO_3$ and doped $BiFeO_3$ films on the $Pt/Ti/SiO_2/Si$ substrate with $LaNiO_3$ buffer layer were carried out with an RF sputtering power of 40W at 400 °C for 2 h under a 3:1 Ar/O_2 flow ratio. After the deposition, the films were cooled to the room temperature in vacuum chamber. Then, the resultant films were annealed at 550 °C for 30 min in air. The top platinum electrodes with a size of 3.14×10^{-4} cm^2 were deposited by DC magnetron sputtering before the electric properties testing. During electrical measurements, positive bias is defined as the current flow from the top electrode to the bottom electrode. In the present study, pure $BiFeO_3$, 4.5 wt % $LiNbO_3$-doped $BiFeO_3$, 9 wt % $LiNbO_3$-doped $BiFeO_3$, and 14.5 wt % $LiNbO_3$-doped $BiFeO_3$ thin films are termed S1, S2, S3, and S4, respectively.

The XRD experiments were performed using Cu Kα radiation on an X'pert diffractometer at 40 kV and 40 mA, including the phase structure and rocking curve studies. The surface and cross-sectional morphologies of pure and doped $BiFeO_3$ thin films were characterized by atomic force microscopy (CSPM5600 of Benyuan) and scanning electron microscopy (Helios Nanolab600i), respectively. The domain structures of pure and doped $BiFeO_3$ thin films were obtained by the modified commercial atomic force microscope (AFM) with a piezoelectric force microscope (PFM) mode (Bruker multimode 8). The piezoelectric response signals from vertical cantilever deflection are proportional to the out-of-plane polarization. The frequency dependence of the dielectric permittivity and dielectric loss was characterized by the Agilent 4294A precision impedance analyzer at the frequencies ranging from 500 Hz to 1 MHz. The leakage current behaviors and P−E hysteresis loops of the samples were measured using a Ferroelectric Measurement System (P-LC100, Radiant Technology). The converse piezoelectric coefficients d_{33} of pure and doped $BiFeO_3$ thin films were characterized using a commercial scanning force microscope (CSPM5600 of Benyuan) equipped with a lock-in amplifier (model SR530, Standford Research System, Inc.) with the same method as that previously reported.[4,26]

3. RESULTS AND DISCUSSION

The XRD patterns of S1, S2, S3, and S4 thin films measured at room temperature are shown in Figure 1. It can be observed from Figure 1a that all of the thin films are well crystallized without detectable impurities or other phases, which indicates that $LiNbO_3$ has been well-doped into the perovskite $BiFeO_3$. Furthermore, only (010) and (020) reflections of $BiFeO_3$ can be clearly observed in all films except for S1 (a small portion of (110) can be found), which suggests that all of the films are highly (010)-oriented. To further evaluate the misorientation degree of S1, S2, S3, and S4 films, we show the measured and

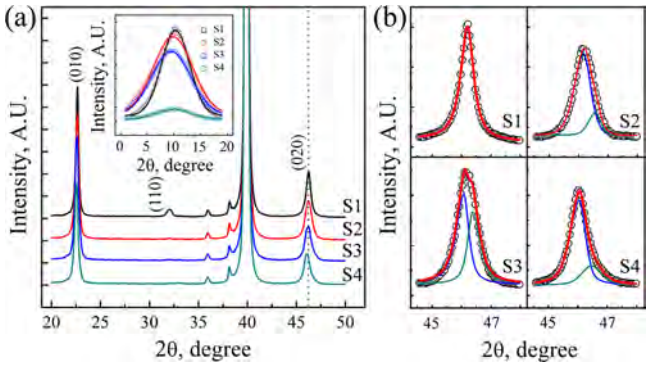

Figure 1. (a) θ−2θ scan XRD patterns of S1, S2, S3, and S4 thin films; the inset is the ω-scan XRD (rocking curve) patterns of S1, S2, S3, and S4 thin films. (b) Measured and fitted profiles of (020) reflections of S1, S2, S3, and S4 thin films.

Gaussian-fitted XRD rocking curves for (010) reflection in the inset in Figure 1a. The Gaussian widths (fwhm) for all of the films are about 6.5−8.5°, which further indicates that all of the films obtained in the present study are highly (010)-oriented. The results above suggest that $LaNiO_3$ buffer layer is very beneficial to the preferential nucleation of $BiFeO_3$, which is consistent with previous reports.[37]

In addition, it can be found from Figure 1a that the positions of (020) reflection for S1, S2, S3, and S4 films gradually shift to a lower angel with $LiNbO_3$ contents increasing. Taking ionic radius and valences into consideration, it is believed that both Li^+ and Nb^{5+} have a larger ionic radius than that of Fe^{3+}, and the substitution of Li^+ and Nb^{5+} for Fe^{3+} will induce a compressive strain (chemical pressure) in the $BiFeO_3$ film and maintain the local charge neutrality. The compressive strain in the $BiFeO_3$ film caused by the Li^+ and Nb^{5+} substitution is in accordance with the shifting reflection positions. Moreover, the profile of (020) reflection of S1 thin film is symmetric, while the (020) reflection profiles of doped $BiFeO_3$ (S2, S3, and S4) thin films are asymmetric. To investigate the differences above clearly, we show the measured and fitted profiles of (020) reflections (using pseudocubic coordinate system) of S1, S2, S3, and S4 films in Figure 1b. It has been well established that for the R phase of $BiFeO_3$ the profile of (020) reflection is singlet, whereas for the T-like phase the (020) reflection profiles are doublet.[38] According to the result above, it can be observed clearly from Figure 1b that the phase structure of S1 film is R because the profile of (010) reflection for S1 film is a symmetric singlet. Meanwhile, the profiles of (010) reflection for doped $BiFeO_3$ (S2, S3, and S4) films are asymmetric and they can split into two different peaks, indicating that a phase transition has taken place in the S2, S3, and S4 films due to the ion substitution. It has been reported that T-like can be induced by epitaxial strain[5] or chemical pressure[17] in the $BiFeO_3$ film. Therefore, the phase structure of S2, S3, and S4 films might be considered as a T-like phase. In other words, the phase structures of S2, S3, and S4 films undergo a change from the high-symmetry R phase to the low-symmetry T-like phase.

The surface and cross-section micrographs of S1, S2, S3, and S4 films are shown in Figure 2. It can be observed from the surface micrographs (Figure 2a,c,e,g) that all of the films exhibit dense, uniform microstructures and small surface roughness. From the cross-section micrographs (Figure 2b,d,f,h) the thicknesses of S1, S2, S3, and S4 films are 295, 280, 360, and 340 nm, respectively. Thus, all S1, S2, S3, and S4 films have a

www.spm.com.cn

DOI: 10.1021/acs.jpcc.5b12291
J. Phys. Chem. C 2016, 120, 6246−6251

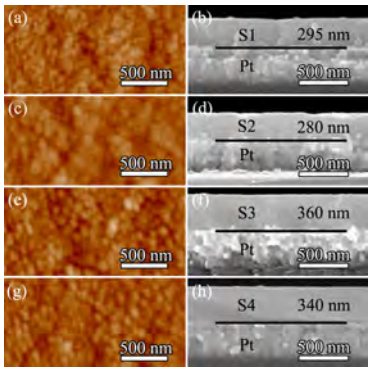

Figure 2. Surface and cross-section micrographs of (a,b) S1 thin film, (c,d) S2 thin film, (e,f) S3 thin film, and (g,h) S4 thin film.

densely packed and homogeneous microstructure on a microscopic scale, indicating that the microstructures of S1, S2, S3, and S4 films are not affected by the doping of $LiNbO_3$. Meanwhile, $LaNiO_3$ buffer layer with a thickness of 10 nm is not observed in the SEM results, which is characterized by the X-ray reflectivity (XRR) in our previous report.[36] From the cross-sectional micrographs (Figure 2b,d,f,h), it is worth noting that the interface between the $BiFeO_3$ film and substrate (Pt) can be clearly distinguished owing to the existence of $LaNiO_3$ buffer layer, which is different from the direct contact between $BiFeO_3$ and Pt.[26]

The dielectric properties of S1, S2, S3, and S4 films shown in Figure 3a were measured at room temperature with the frequency ranging from 500 Hz to 1 MHz. From Figure 3a, it can be observed that the dielectric constants of S1, S2, S3, and S4 films increase first and then decrease with $LiNbO_3$ contents increasing. More importantly, the dielectric losses of S2 and S3 films are much lower than that of pure $BiFeO_3$ (S1) film at a frequency ranging from 500 Hz to 1 MHz; however, the dielectric loss of S4 film, which is comparable to that of pure $BiFeO_3$ (S1) film, especially at low frequencies, as shown inset in Figure 3a, is much higher than that of S2 and S3 films.

To assess the leakage behavior of pure and doped $BiFeO_3$ film, the leakage current (I) versus electric field (E) curves of S1, S2, S3, and S4 films were investigated at room temperature, and the results are shown in Figure 3b. It is observed from Figure 3b) that pure $BiFeO_3$ (S1) film shows a high leakage current; meanwhile, the $LiNbO_3$-doped $BiFeO_3$ (S2, S3, and S4) films exhibit greatly reduced leakage current. The reduced dielectric loss and leakage current are caused by the following reasons: first, the substitution of Li^{+} and Nb^{5+} into the Fe site attributes to eliminate oxygen vacancies; second, the introduction of $LaNiO_3$ buffer layer prevents the interface reaction between platinum and bismuth, which is of benefit to reduce Bi deficiencies.

More importantly, it can be observed clearly from the upper inset in Figure 3b that a unidirectional conductive feature can be found in the S3 film; namely, it is conductive under positive biases and less-conductive under negative biases. To further confirm the unidirectional conductive feature, we show the corresponding currents (absolute value) of S1, S2, S3, and S4 films at 200 and −200 kV/cm in the lower inset in Figure 3b. From the lower inset figure in Figure 3b, it can be seen that the corresponding currents (absolute value) of the doped $BiFeO_3$ (S2, S3, and S4) films at 200 and −200 kV/cm exhibit large discrepancies, especially for the S3 film; however, for the pure $BiFeO_3$ (S1) film, the discrepancy is not existent. The results

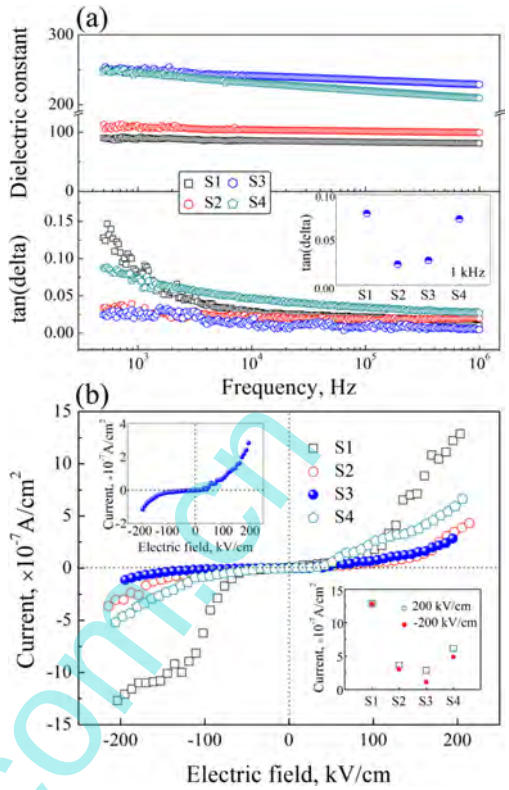

Figure 3. (a) Frequency dependence of dielectric permittivity and dielectric loss; the inset is the dielectric losses of S1, S2, S3, and S4 thin films at 1 kHz. (b) $I-V$ curves for S1, S2, S3, and S4 thin films. Upper inset is the $I-V$ curve for S2 thin film, and lower inset is the corresponding current (absolute value) for S1, S2, S3, and S4 thin films at 200 and −200 kV/cm, respectively.

above suggest that the doped $BiFeO_3$ (S2, S3, and S4) films show a unidirectional conductive feature, while the pure $BiFeO_3$ (S1) film does not show any rectifying feature.

In general, the diode-like rectifying feature is relevant to a built-in electric field generated by the energy band bending or self-polarization effect.[32,39] In the present system, there are no differences in the configuration of pure $BiFeO_3$ (S1) and doped $BiFeO_3$ (S2, S3, and S4) films. Therefore, the diode-like rectifying features in the doped $BiFeO_3$ (S2, S3, and S4) films are not caused by the energy band bending, which may be caused by the self-polarization effects. To further investigate the out-of-plane domain structures (upward or downward) of highly (010)-oriented S1, S2, S3, and S4 films, we performed the PFM image analysis without prepolarization. The representative out-of-plane PFM images recorded on the S1, S2, S3, and S4 films are shown in Figure 4, where the bright domains represent the upward polarizations and dark domains mean the downward or in-plane polarizations.

Figure 4a shows the domain structures of pure $BiFeO_3$ (S1) film; it can be clearly found that the unpoled S1 film consists of many nanodomains with different polarizations, and the portions of bright and dark domains in the S1 film are almost equal to each other.

Meanwhile, it can be seen from Figure 4b–d that the majority of the domains of the doped $BiFeO_3$ (S2, S3, and S4) films are oriented with the upward polarization (yellow bright). It is worth noting that the domain structures of the unpoled S3 film are almost upward polarization (close to the out-of-plane direction), as shown in Figure 4c, indicating an upward self-

www.xjtu.com.cn

DOI: 10.1021/acs.jpcc.5b12291
J. Phys. Chem. C 2016, 120, 6246−6251

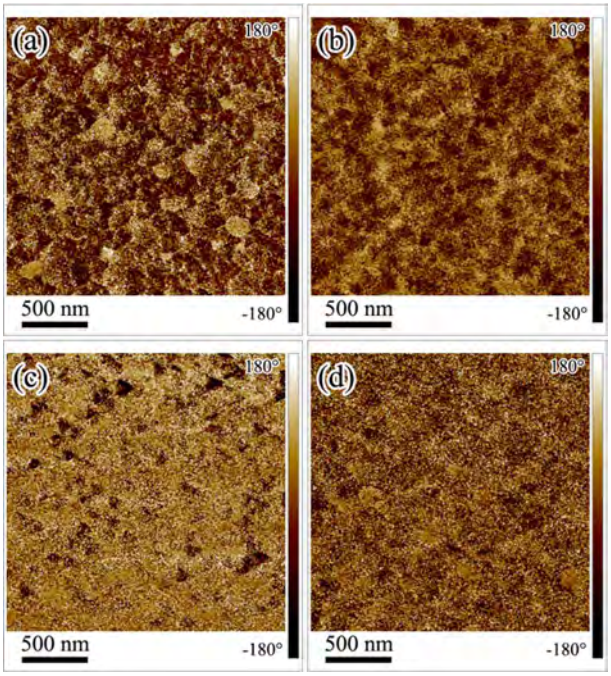

Figure 4. PFM domain structures of (a) the S1 thin film, (b) the S2 thin film, (c) the S3 thin film, and (d) the S4 thin film.

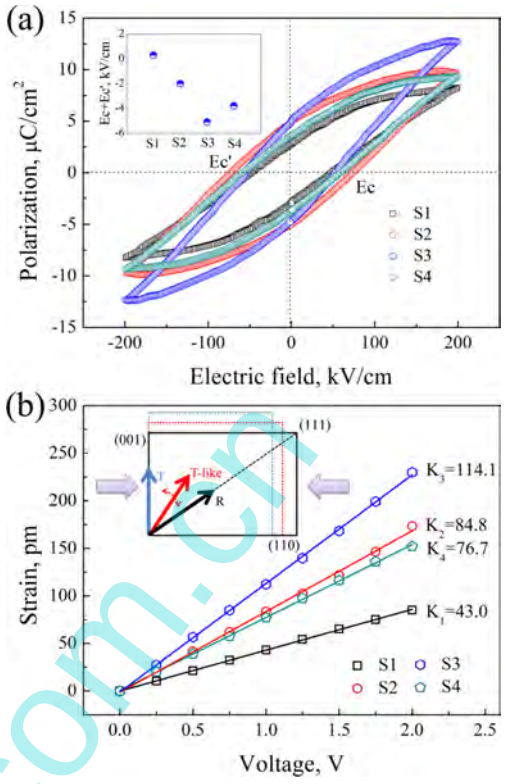

Figure 5. (a) *P*–*E* hysteresis loops of S1, S2, S3, and S4 thin films. The inset is the sum of corresponding positive and negative coercive fields for S1, S2, S3, and S4 thin films. (b) Converse piezoelectric coefficient (d_{33}) of S1, S2, S3, and S4 thin films, where the slope (K) represents d_{33}; the inset is the schematic of polarization rotation path of R, T, and T-like phase.

polarization phenomenon according to previous reports.[31] Besides, the upward self-polarization phenomena also exist in S2 and S4 films, as shown in Figure 4b,d. It has been reported that the conductivity of certain domain walls of the $BiFeO_3$ film, especially for the 180° domain wall, is much higher than that of domains themselves.[27] In the present study, the density of domain walls in the doped $BiFeO_3$ (S2, S3, and S4) films is much less than that of the pure $BiFeO_3$ (S1) film, which also contributes to the reduced leakage in the doped $BiFeO_3$ (S2, S3, and S4) films. Taking all of the above into consideration, it can be concluded that the diode-like rectifying features in the doped $BiFeO_3$ (S2, S3, and S4) films are caused by the self-polarization effect.

In the present study, there is a large compressive strain and T-like phase in the doped $BiFeO_3$ (S2, S3, and S4) films as previously discussed. It has been reported that upward self-polarizations can be derived from the inhomogeneous compressive strain.[31,32] Therefore, the upward self-polarization formed in the doped $BiFeO_3$ film is mainly caused by the compressive strain, which can mechanically switch the polarization of $BiFeO_3$ film.[32] Furthermore, the local electric fields (E_D) formed by the Li^+-Nb^{5+} pairs may also contribute to the upward self-polarization in the doped $BiFeO_3$ films if the pairs are in directional arrangement.

The ferroelectric polarization versus electric-field curves (*P*–*E* hysteresis loops) of S1, S2, S3, and S4 films shown in Figure 5a were measured at 1 kHz at room temperature. From Figure 5a, the slant *P*–*E* loop and low remnant polarization (P_r) of pure $BiFeO_3$ (S1) film are caused by the large leakage current and nonuniformity of domains. Meanwhile, in the doped $BiFeO_3$ films, the ferroelectric responses are greatly enhanced, especially for the S3 films. In addition, the sum of corresponding positive and negative coercive fields for S1, S2, S3, and S4 thin films is shown in the inset in Figure 5a. It can be observed from the inset in Figure 5a that the built-in electric fields exist in doped $BiFeO_3$ (S2, S3 and S4) films because of the unequal positive and negative coercive field, which is in accordance with the upward self-polarization effect. The enhanced ferroelectricities of doped $BiFeO_3$ films are the coupling results of reduced leakage currents and low densities of domain walls because the coupling effects allow domains to switch effectively under sufficient high electric fields.

Furthermore, the measured and linear fitted converse piezoelectric coefficients (d_{33}) of pure and doped $BiFeO_3$ films are shown in Figure 5b, where the slope of fitted lines represents d_{33} of the samples.[3,4] From Figure 5b, it can be observed that the d_{33} value of pure $BiFeO_3$ (S1) film is only 43.0 pm/V (K_1 shown in Figure 5b). Although there are many nanodomains, the weak piezoelectric response of pure $BiFeO_3$ film is derived from the large leakage current and limited rotation of the spontaneous polarization vector of R phase.[40] The d_{33} value of S2 film is 84.8 pm/V (K_2 shown in Figure 5b), which is almost twice as that of S1 film. With the same film thickness of S1 and S2 films, the enhancement of piezoelectric response of S2 film compared with S1 film is derived from the low-symmetry phase induced by doping, which will be discussed later. With $LiNbO_3$ contents increasing, the piezoelectric response of doped $BiFeO_3$ films is greatly enhanced, as shown in Figure 5b. S3 film exhibits the highest d_{33} value of 114.1 pm/V (K_3 in the Figure 5b), which is comparable to that of the lead-based piezoelectric films.[7] Similar to the dielectric and ferroelectric properties, the piezoelectric response of doped $BiFeO_3$ films decreases with the further increasing of $LiNbO_3$ contents (d_{33} value of S4 film is 76.7 pm/V). With the same thickness of S3 and S4 films, the reduced piezoelectric response

www.sjtu.com.cn

DOI: 10.1021/acs.jpcc.5b12291
J. Phys. Chem. C 2016, 120, 6246–6251

of S4 film is caused by the weak coupling of low-symmetry phase and self-polarization. Compared with S2 and S3 films, the degradations of dielectric, ferroelectric, and piezoelectric properties of S4 film indicate that an optimal doping content (more is not better) exists in the $LiNbO_3$-doped $BiFeO_3$ system.

It is generally acknowledged that the large piezoelectric response is related to the ease of polarization rotation or phase transition under external stimuli. In the present study, the low-symmetry phase (T-like) is found in the doped $BiFeO_3$ (S2, S3, and S4) films, which can serve as a structure bridge between the R and T phases as shown inset in Figure 5b. The bridge facilitating the field-induced phase transition (R−T) can result in a large piezoelectric response in the doped $BiFeO_3$ film. In addition, the polarization vector of the T-like phase can rotate within a monoclinic plane, which is different from that of pure T and R phases.[40] Taking the upward self-polarization into consideration, the polarization vectors of the T-like phase and nanodomains are rotated easily to the direction of external electric field (perpendicular to substrates) under small external stimuli. The coexistences of T-like phases, nanodomains, and upward self-polarizations also contribute to the large piezoelectric response in the doped $BiFeO_3$ films, which is in accordance with the previous reports.[40] Moreover, the reduced leakage current allows the doped $BiFeO_3$ films to be fully polarized, which is also helpful to the large piezoelectric response of doped $BiFeO_3$ films, especially for the S3 film.

4. CONCLUSIONS

In summary, pure $BiFeO_3$ (S1) and Li^+-Nb^{5+}-pair-doped $BiFeO_3$ (S2, S3, and S4) films were prepared by the radio-frequency magnetron sputtering on the $LaNiO_3$-buffered Pt/Ti/SiO_2/Si substrate. Because of the chemical pressure induced by the substitution of larger Li^+ and Nb^{5+} for smaller Fe^{3+}, the phase structure of the doped $BiFeO_3$ films undergoes a change from the high-symmetry R phase to the low-symmetry T-like phase, which is different from the pure $BiFeO_3$ film (R phase). Besides, the upward self-polarization phenomena and reduced leakage current in the highly (010)-oriented $LiNbO_3$-doped $BiFeO_3$ films were also studied. Taking the T-like phase, reduced leakage current, low densities of domain wall, and upward self-polarization into consideration, the doped $BiFeO_3$ films exhibit greatly enhanced dielectric, ferroelectric, and piezoelectric performances. It is worth noting that the S3 film shows an excellent piezoelectricity, with d_{33} value of 114.1 pm/V, which is comparable to that of lead-based piezoelectric films.

AUTHOR INFORMATION

Corresponding Author

*E-mail: wdfei@hit.edu.cn. Fax/Tel: +86-541-86413908.

Notes

The authors declare no competing financial interest.

ACKNOWLEDGMENTS

The research was financially supported by the National Natural Science Foundations of China (Nos. 11272102 and 51471057).

REFERENCES

(1) Nagarajan, V.; Roytburd, A.; Stanishevsky, A.; Prasertchoung, S.; Zhao, T.; Chen, L.; Melngailis, J.; Auciello, O.; Ramesh, R. Dynamics of Ferroelastic Domains in Ferroelectric Thin Films. *Nat. Mater.* **2003**, *2*, 43−47.

(2) Cox, D. E.; Noheda, B.; Shirane, G.; Uesu, Y.; Fujishiro, K.; Yamada, Y. Universal Phase Diagram for High-Piezoelectric Perovskite Systems. *Appl. Phys. Lett.* **2001**, *79*, 400−402.

(3) Ryu, J.; Choi, J. J.; Hahn, B. D.; Park, D. S.; Yoon, W. H. Ferroelectric and Piezoelectric Properties of $0.948(K_{0.5}Na_{0.5})NbO_3$−$0.052LiSbO_3$ Lead-Free Piezoelectric Thick Film by Aerosol Deposition. *Appl. Phys. Lett.* **2008**, *92*, 012905.

(4) Zhao, M. H.; Wang, Z. L.; Mao, S. X. Piezoelectric Characterization of Individual Zinc Oxide Nanobelt Probed by Piezoresponse Force Microscope. *Nano Lett.* **2004**, *4*, 587−590.

(5) Wang, J.; Neaton, J. B.; Zheng, H.; Nagarajan, V.; Ogale, S. B.; Liu, B.; Viehland, D.; Vaithyanathan, V.; Schlom, D. G.; Waghmare, U. V.; et al. Epitaxial $BiFeO_3$ Multiferroic Thin Film Heterostructures. *Science* **2003**, *299*, 1719−1722.

(6) Noheda, B.; Cox, D. E.; Shirane, G.; Guo, R.; Jones, B.; Cross, L. E. Stability of the Monoclinic Phase in the Ferroelectric Perovskite $PbZr_{1-x}Ti_xO_3$. *Phys. Rev. B: Condens. Matter Mater. Phys.* **2000**, *63*, 014103.

(7) Noheda, B.; Cox, D. E.; Shirane, G.; Park, S. E.; Cross, L. E.; Zhong, Z. Polarization Rotation Via a Monoclinic Phase in the Piezoelectric 92%$PbZn_{1/3}Nb_{2/3}O_3$-8% $PbTiO_3$. *Phys. Rev. Lett.* **2001**, *86*, 3891−3894.

(8) Taylor, D. V.; Damjanovic, D. Piezoelectric Properties of Rhombohedral Pb(Zr, Ti)O_3 Thin Films with (100), (111), and "Random" Crystallographic Orientation. *Appl. Phys. Lett.* **2000**, *76*, 1615−1617.

(9) Zeches, R. J.; Rossell, M. D.; Zhang, J. X.; Hatt, A. J.; He, Q.; Yang, C. H.; Kumar, A.; Wang, C. H.; Melville, A.; Adamo, C.; et al. A Strain-Driven Morphotropic Phase Boundary in $BiFeO_3$. *Science* **2009**, *326*, 977−980.

(10) Damodaran, A. R.; Lee, S.; Karthik, J.; MacLaren, S.; Martin, L. W. Temperature and Thickness Evolution and Epitaxial Breakdown in Highly Strained $BiFeO_3$thin Films. *Phys. Rev. B: Condens. Matter Mater. Phys.* **2012**, *85*, 024113.

(11) Dupé, B.; Infante, I. C.; Geneste, G.; Janolin, P. E.; Bibes, M.; Barthélémy, A.; Lisenkov, S.; Bellaiche, L.; Ravy, S.; Dkhil, B. Competing Phases in $BiFeO_3$thin Films under Compressive Epitaxial Strain. *Phys. Rev. B: Condens. Matter Mater. Phys.* **2010**, *81*, 144128.

(12) Vasudevan, R. K.; Liu, Y.; Li, J.; Liang, W. I.; Kumar, A.; Jesse, S.; Chen, Y. C.; Chu, Y. H.; Nagarajan, V.; Kalinin, S. V. Nanoscale Control of Phase Variants in Strain-Engineered $BiFeO_3$. *Nano Lett.* **2011**, *11*, 3346−3354.

(13) Damodaran, A. R.; Liang, C. W.; He, Q.; Peng, C. Y.; Chang, L.; Chu, Y. H.; Martin, L. W. Nanoscale Structure and Mechanism for Enhanced Electromechanical Response of Highly Strained $BiFeO_3$ Thin Films. *Adv. Mater.* **2011**, *23*, 3170−3175.

(14) Chen, Z. H.; Luo, Z. L.; Huang, C. W.; Qi, Y. J.; Yang, P.; You, L.; Hu, C. S.; Wu, T.; Wang, J. L.; Gao, C.; et al. Low-Symmetry Monoclinic Phases and Polarization Rotation Path Mediated by Epitaxial Strain in Multiferroic $BiFeO_3$ Thin Films. *Adv. Funct. Mater.* **2011**, *21*, 133−138.

(15) Rossell, M. D.; Erni, R.; Prange, M. P.; Idrobo, J. C.; Luo, W.; Zeches, R. J.; Pantelides, S. T.; Ramesh, R. Atomic Structure of Highly Strained $BiFeO_3$ Thin Films. *Phys. Rev. Lett.* **2012**, *108*, 047601.

(16) Wu, Z.; Cohen, R. Pressure-Induced Anomalous Phase Transitions and Colossal Enhancement of Piezoelectricity in $PbTiO_3$. *Phys. Rev. Lett.* **2005**, *95*, 037601.

(17) Kan, D.; Anbusathaiah, V.; Takeuchi, I. Chemical Substitution-Induced Ferroelectric Polarization Rotation in $BiFeO_3$. *Adv. Mater.* **2011**, *23*, 1765−1769.

(18) Chen, X.; Hu, G.; Wu, W.; Yang, C.; Wang, X.; Fan, S. Large Piezoelectric Coefficient in Tb-Doped $BiFeO_3$films. *J. Am. Ceram. Soc.* **2010**, *93*, 948−950.

(19) Cheng, Z.; Wang, X.; Dou, S.; Kimura, H.; Ozawa, K. Improved Ferroelectric Properties in Multiferroic $BiFeO_3$thin Films through La and Nb Codoping. *Phys. Rev. B: Condens. Matter Mater. Phys.* **2008**, *77*, 092101.

(20) Fujino, S.; Murakami, M.; Anbusathaiah, V.; Lim, S. H.; Nagarajan, V.; Fennie, C. J.; Wuttig, M.; Salamanca-Riba, L.; Takeuchi,

www.sjpm.com.cn

DOI: 10.1021/acs.jpcc.5b12291
J. Phys. Chem. C 2016, 120, 6246−6251

I. Combinatorial Discovery of a Lead-Free Morphotropic Phase Boundary in a Thin-Film Piezoelectric Perovskite. *Appl. Phys. Lett.* **2008**, *92*, 202904.
(21) Gao, F.; Cai, C.; Wang, Y.; Dong, S.; Qiu, X. Y.; Yuan, G. L.; Liu, Z. G.; Liu, J. M. Preparation of La-Doped $BiFeO_3$ Thin Films with Fe^{2+} Ions on Si Substrates. *J. Appl. Phys.* **2006**, *99*, 094105.
(22) Yan, F.; Zhu, T. J.; Lai, M. O.; Lu, L. Enhanced Multiferroic Properties and Domain Structure of La-Doped $BiFeO_3$ Thin Films. *Scr. Mater.* **2010**, *63*, 780−783.
(23) Yu, B. F.; Li, M. Y.; Liu, J.; Guo, D. Y.; Pei, L.; Zhao, X. Z. Effects of Ion Doping at Different Sites on Electrical Properties of Multiferroic $BiFeO_3$ Ceramics. *J. Phys. D: Appl. Phys.* **2008**, *41*, 065003.
(24) Wang, D. H.; Yan, L.; Ong, C. K.; Du, Y. W. $BiFeO_3$ Film Deposited on Si Substrate Buffered with $La_{0.7}Sr_{0.3}MnO_3$ Electrode. *Appl. Phys. Lett.* **2006**, *89*, 182905.
(25) Huang, F.; Lu, X.; Lin, W.; Cai, W.; Wu, X.; Kan, Y.; Sang, H.; Zhu, J. Multiferroic Properties and Dielectric Relaxation of $BiFeO_3$/$Bi_{3.25}La_{0.75}Ti_3O_{12}$ Double-Layered Thin Films. *Appl. Phys. Lett.* **2007**, *90*, 252903.
(26) Hou, Y. F.; Li, W. L.; Zhang, T. D.; Wang, W.; Cao, W. P.; Liu, X. L.; Fei, W. D. Large Piezoelectric Response of $BiFeO_3$/$BaTiO_3$ Polycrystalline Films Induced by the Low-Symmetry Phase. *Phys. Chem. Chem. Phys.* **2015**, *17*, 11593−11597.
(27) Yan, F.; Lai, M. O.; Lu, L.; Zhu, T. J. Enhanced Multiferroic Properties and Valence Effect of Ru-Doped $BiFeO_3$ Thin Films. *J. Phys. Chem. C* **2010**, *114*, 6994−6998.
(28) Kim, J. K.; Kim, S. S.; Kim, W. J.; Bhalla, A. S.; Guo, R. Y. Enhanced Ferroelectric Properties of Cr-Doped $BiFeO_3$ Thin Films Grown by Chemical Solution Deposition. *Appl. Phys. Lett.* **2006**, *88*, 132901.
(29) Chu, Y. H.; He, Q.; Yang, C. H.; Yu, P.; Martin, L. W.; Shafer, P.; Ramesh, R. Nanoscale Control of Domain Architectures in $BiFeO_3$ Thin Films. *Nano Lett.* **2009**, *9*, 1726−1730.
(30) Hou, Y. F.; Zhang, T. D.; Li, W. L.; Cao, W. P.; Yu, Y.; Xu, D.; Wang, W.; Liu, X. L.; Fei, W. D. Self-Polarization Induced by Lattice Mismatch and Defect Dipole Alignment in (001) $BaTiO_3$/$LaNiO_3$ Polycrystalline Film Prepared by Magnetron Sputtering at Low Temperature. *RSC Adv.* **2015**, *5*, 61821−61827.
(31) Chen, J.; Luo, Y.; Ou, X.; Yuan, G.; Wang, Y.; Yang, Y.; Yin, J.; Liu, Z. Upward Ferroelectric Self-Polarization Induced by Compressive Epitaxial Strain in (001) $BaTiO_3$ Films. *J. Appl. Phys.* **2013**, *113*, 204105.
(32) Chen, X. M.; Zou, Y. H.; Yuan, G. L.; Zeng, M.; Liu, J. M.; Yin, J.; Liu, Z. G. Temperature Gradient Introduced Ferroelectric Self-Poling in $BiFeO_3$ceramics. *J. Am. Ceram. Soc.* **2013**, *96*, 3788−3792.
(33) Wang, Z.; Zhang, X. X.; Wang, X.; Yue, W.; Li, J.; Miao, J.; Zhu, W. Giant Flexoelectric Polarization in a Micromachined Ferroelectric Diaphragm. *Adv. Funct. Mater.* **2013**, *23*, 124−132.
(34) Xu, D.; Li, W. L.; Wang, L. D.; Wang, W.; Cao, W. P.; Fei, W. D. Large Piezoelectric Properties Induced by Doping Ionic Pairs in $BaTiO_3$ Ceramics. *Acta Mater.* **2014**, *79*, 84−92.
(35) Xu, D.; Wang, L. D.; Li, W. L.; Wang, W.; Hou, Y. F.; Cao, W. P.; Feng, Y.; Fei, W. D. Enhanced Piezoelectric and Mechanical Properties of AlN-Modified $BaTiO_3$ Composite Ceramics. *Phys. Chem. Chem. Phys.* **2014**, *16*, 13078−13085.
(36) Li, W. L.; Zhang, T. D.; Xu, D.; Hou, Y. F.; Cao, W. P.; Fei, W. D. $LaNiO_3$ Seed Layer Induced Enhancement of Piezoelectric Properties in (100)-Oriented (1−x)BZT−xBCT Thin Films. *J. Eur. Ceram. Soc.* **2015**, *35*, 2041−2049.
(37) Lee, Y. H.; Wu, J. M.; Chueh, Y. L.; Chou, L. J. Low-Temperature Growth and Interface Characterization of $BiFeO_3$ Thin Films with Reduced Leakage Current. *Appl. Phys. Lett.* **2005**, *87*, 172901.
(38) Zhang, S. Q.; Wang, L. D.; Li, W. L.; Li, N.; Fei, W. D. Effects of Lanthanum Doping on the Preferred Orientation, Phase Structure and Electrical Properties of Sol−Gel Derived $Pb_{1-3x/2}La_x(Zr_{0.6}Ti_{0.4})O_3$ Thin Films. *J. Alloys Compd.* **2011**, *509*, 2976−2980.
(39) Wang, C. C.; Liu, G. Z.; He, M.; Lu, H. B. Low-Frequency Negative Capacitance in $La_{0.8}Sr_{0.2}MnO_3$/Nb-Doped $SrTiO_3$ Heterojunction. *Appl. Phys. Lett.* **2008**, *92*, 052905.
(40) Chen, Z.; Prosandeev, S.; Luo, Z. L.; Ren, W.; Qi, Y. J.; Huang, C. W.; You, L.; Gao, C.; Kornev, I. A.; Wu, T.; et al. Coexistence of Ferroelectric Triclinic Phases in Highly Strained $BiFeO_3$films. *Phys. Rev. B: Condens. Matter Mater. Phys.* **2011**, *84*, 094116.

www.spm.com.cn

DOI: 10.1021/acs.jpcc.5b12291
J. Phys. Chem. C 2016, 120, 6246−6251